

## DEVELOPING CANADA'S FIRST PORTABLE QUANTUM GRAVIMETER

**SUMMARY:** We discuss the development of Canada's first portable quantum gravimeter for applications in natural resource prospecting, geophysics, positioning, and navigation.



By **TIMOTHY HUNT** <timothy.hunt@unb.ca>, **CRISTIAN RAMIREZ RODRIGUEZ** <cristian.ramirez@unb.ca>, and **BRYNLE BARRETT** <brynle.barrett@unb.ca>

Dept. of Physics, University of New Brunswick,  
8 Bailey Dr., Fredericton, NB, E3B 5A3, Canada

**N**atural resources such as water, minerals, and petroleum can be detected passively using sensitive gravimeters that measure local variations in gravity. Gravimeters are used in mining and resource exploration to detect subsurface density variations that indicate critical mineral reserves. They are crucial for geodesists to determine geodetic heights referenced to sea level, or water levels in the Great Lakes, which strongly affect the shipping industry [1]. Gravimeters are also essential to geophysicists for detecting dynamic mass transport phenomena, including tectonic uplift due to glacial recession [2], volcanic activity [3, 4], solid-Earth tides and ocean loading effects [5]. The Canadian Geodetic Survey Division at NRCan has a vital need for precise and stable absolute gravimeters to replace its aging fleet of “classical” instruments.

Classical free-fall gravimeters operate using an optical Michelson interferometer with a free-falling corner-cube reflector as the test mass [6]. Although they have been the industry standard since the 1990s, classical gravimeters are prone to long-term drift and require periodic recalibration/repair due to mechanical wear and tear. For example, the Micro-G LaCoste FG5-X requires servicing after  $10^6$  drops (or after  $\sim 16$  weeks at 10 s per drop) [7]. Quantum gravimeters have only recently emerged on the market [8, 9]. These devices are the quantum analog of classical free-fall gravimeters: they use a cloud of laser-cooled atoms instead of a macroscopic test mass. They are also self-referenced to quantum properties of the atoms; thus, they do not require recalibration, have no moving parts, consume less power, have a higher repetition rate (2 Hz or 0.5 s per drop), and can be operated remotely without intervention for years. These features make quantum gravimeters attractive for remote monitoring applications operated by non-expert users.

Canadian academics and high-tech companies continue to make important contributions to quantum sensing technologies [10], but there has been surprisingly little work on cold-atom-based gravimeters in Canada [11-13]. Several countries have developed portable atomic gravimeters (e.g., France [14], USA [15], China [16], Germany [17], United Kingdom [18], Singapore [19]), with some already offering

commercial products [9]. NRCan recently acquired an Exail AQG (model B13) as part of Canada's growing investment in quantum technology, but at \$750k CAD per unit the current cost makes widespread deployment prohibitive.

Cold-atom-based gravimeters have been operated on moving vehicles and successfully produced high-resolution gravity maps [20, 21]. Real-time gravity data is a crucial component of autonomous (GPS-free) navigation systems, which ensure robust positioning in the presence of adversarial spoofing or jamming. The Department of National Defence (DND) has identified quantum sensors as a critical technology for the defence and security of Canada and her allies. Thus, developing sovereign quantum sensing technology is both timely and necessary.

In this article, we present progress toward the development of two quantum gravimeters at the University of New Brunswick (UNB): a 1<sup>st</sup>-generation table-top instrument that will act as a high-accuracy gravity reference, and a 2<sup>nd</sup>-generation field-deployable instrument – the first portable quantum gravimeter designed and built in Canada.

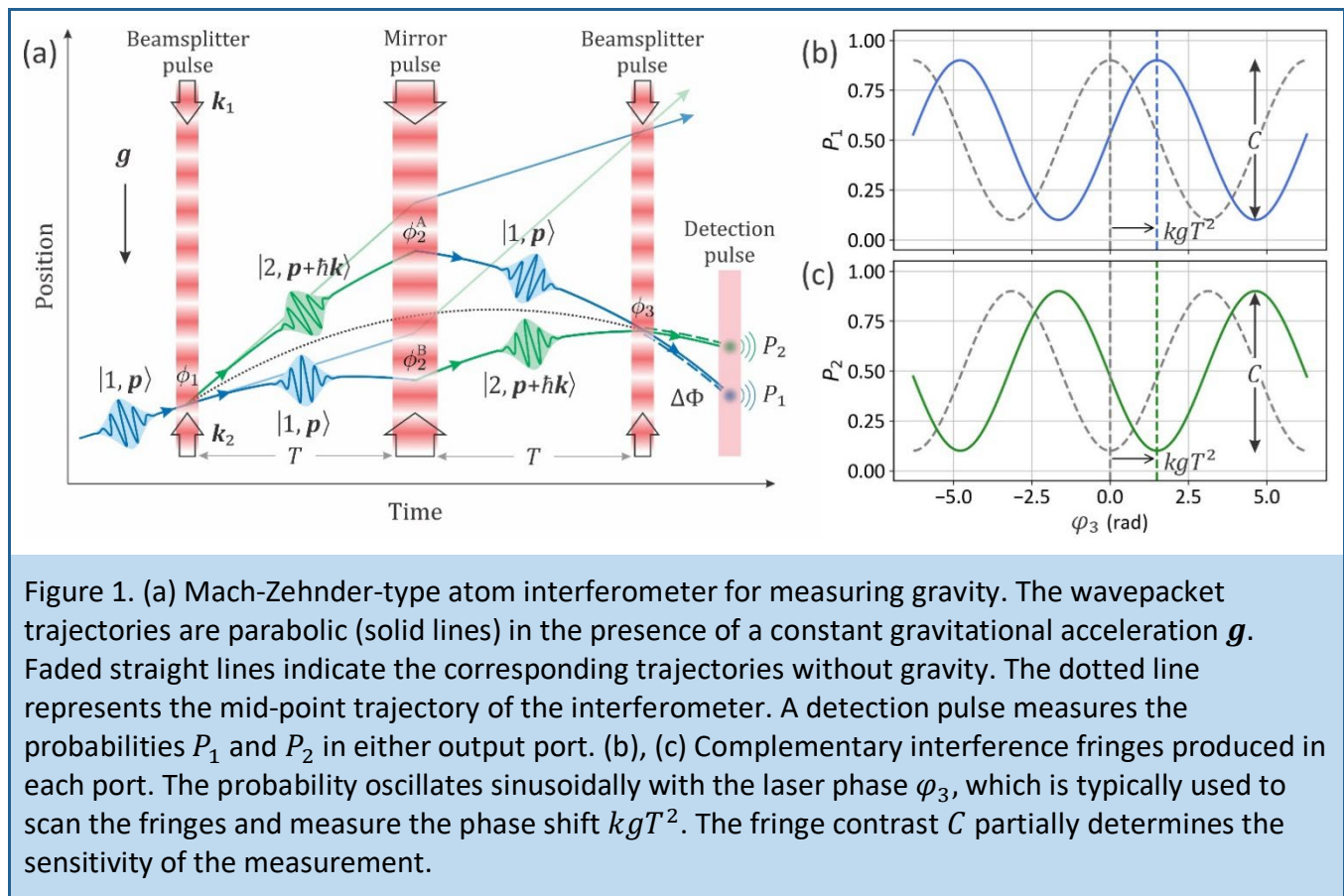
## MEASURING GRAVITY WITH MATTER-WAVE INTERFEROMETRY

A cornerstone of quantum mechanics is the wave-particle duality of matter: all building blocks of matter (electrons, quarks, protons, atoms, etc.) can behave as both particles and waves. An atom moving relative to an observer can be represented as a “wavepacket” with a so-called de Broglie wavelength that is inversely proportional to its mass and velocity. Here, the amplitude of the wavepacket at any point in space represents the probability of finding the atom at that point. A quantum gravimeter relies on the interference between two atomic wavepackets in a **matter-wave interferometer**: the analog of an optical interferometer where the roles of light and matter are reversed.

Figure 1 depicts the matter-wave interferometer most widely used to measure gravity: the Mach-Zehnder configuration [22]. This atom interferometer relies on the coherent transfer of photon momentum to the atoms using optical Raman transitions between two long-lived ground states  $|1\rangle$  and  $|2\rangle$ . Light pulses stimulate atoms in state  $|1\rangle$  to absorb a photon along one direction  $\mathbf{k}_1$  and emit a photon along the opposite direction  $\mathbf{k}_2$ —causing a transition to state  $|2\rangle$ . During this process, the atom “recoils” and picks up two photons of momentum:  $\hbar\mathbf{k} = \hbar(\mathbf{k}_1 - \mathbf{k}_2)$ . The Mach-Zehnder configuration consists of three light pulses, each separated by a free-fall time  $T$ , as shown in Fig. 1(a). The first pulse carries out the role of a beamsplitter in an optical interferometer, which creates an equal superposition of the two states. The second light pulse acts as a mirror, exchanging the population between the two states and redirecting the wavepackets back toward one another. The final beamsplitter pulse recombines the wavepackets by “closing” the interferometer pathways—causing them to interfere. This generates two possible output “ports” where the atom can be found, one corresponding to state  $|1\rangle$  with probability  $P_1 = |\langle 1|\psi\rangle|^2$ , and the other to state  $|2\rangle$  with probability  $P_2 = |\langle 2|\psi\rangle|^2$ . These probabilities can be measured with a resonant detection pulse, as shown in Fig. 1(a). This leads to complementary interference fringes in the probabilities:  $P_{1,2} = \frac{1}{2}(1 \pm C \cos \Delta\Phi)$ , where  $C$  is the contrast of the interference fringes, as shown in Figs. 1(b) and 1(c). The total phase shift

$\Delta\Phi$  is given by the sum of the laser phases  $\phi_i = \mathbf{k} \cdot \mathbf{r}(t_i) + \phi_i$  imprinted on the atoms along the mid-point trajectory of the interferometer:  $\Delta\Phi = \mathbf{k} \cdot \mathbf{g} T^2$  [23], where  $T$  is the free-fall time between light pulses.

Since this phase scales as  $kT^2$ , and  $k \approx 4\pi/\lambda \sim 10^7$  rad/m for commonly used transitions in alkali-metal atoms, very precise measurements of  $g$  can be obtained by measuring this phase shift for large  $T$  [24]. Assuming a single-measurement phase uncertainty of  $\delta\Phi \approx 10^{-2}$  rad at  $T = 100$  ms, the corresponding relative uncertainty in gravity is  $\delta g/g = \delta\Phi/kgT^2 \approx 10^{-8}$ . With averaging, this precision reaches below  $10^{-9}$  after a few hundred measurements under quiet conditions [25]. Instruments capable of this sensitivity can observe gravity signals produced by a large range of geophysical phenomena [2].



## QUANTUM GRAVIMETER DESIGN

Two quantum gravimeters are being developed in the Quantum Sensing and Ultracold Matter Lab at UNB. Figure 2 depicts the sensor heads, which each consist of an ultra-high vacuum (UHV) system, various optical elements, and laser beams for cooling and manipulating rubidium atoms. Quantum

Gravimeter 1.0 (QG1) is a stationary, table-top instrument designed to reach a sensitivity of  $1 \times 10^{-8} g$  at 1 s of integration time, and an accuracy around  $10^{-9} g$ . The objective of QG1 is to act as one of Canada's primary gravity standards—providing uninterrupted high-accuracy time-variable gravity data for long timescales and traceability for gravimetric/geodetic heights, while also serving as an accurate calibration reference for other gravimeters/accelerometers.

The 6.8-L sensor head shown in Fig. 2(a) consists of two main chambers: a glass cell, and a central titanium “science chamber”. The glass cell houses a dispenser that produces hot rubidium vapour that we laser cool in a 2D magneto-optical trap (MOT) [26]. These cold atoms are then optically “pushed” through a small pinhole—creating a cold atomic beam in the science chamber. In the science chamber, the atoms are loaded into a 3D MOT (approximately  $10^9$  atoms in 1 s) and further cooled to a temperature of a few micro-Kelvin ( $10^{-6}$  K). An interferometry beam is aligned vertically through the science chamber to ensure the atomic cloud maintains overlap with the laser as it falls. Two stainless-steel cubes are fixed above and below the science chamber to provide an extended free-fall height up to 0.5 m—corresponding to  $T \approx 300$  ms in an atomic fountain geometry. Finally, two near-resonance light sheets at the bottom of the science chamber serve as detection beams to count the number of atoms in states  $|1\rangle$  and  $|2\rangle$ , and hence the probabilities  $P_1$  and  $P_2$  in each interferometer port.

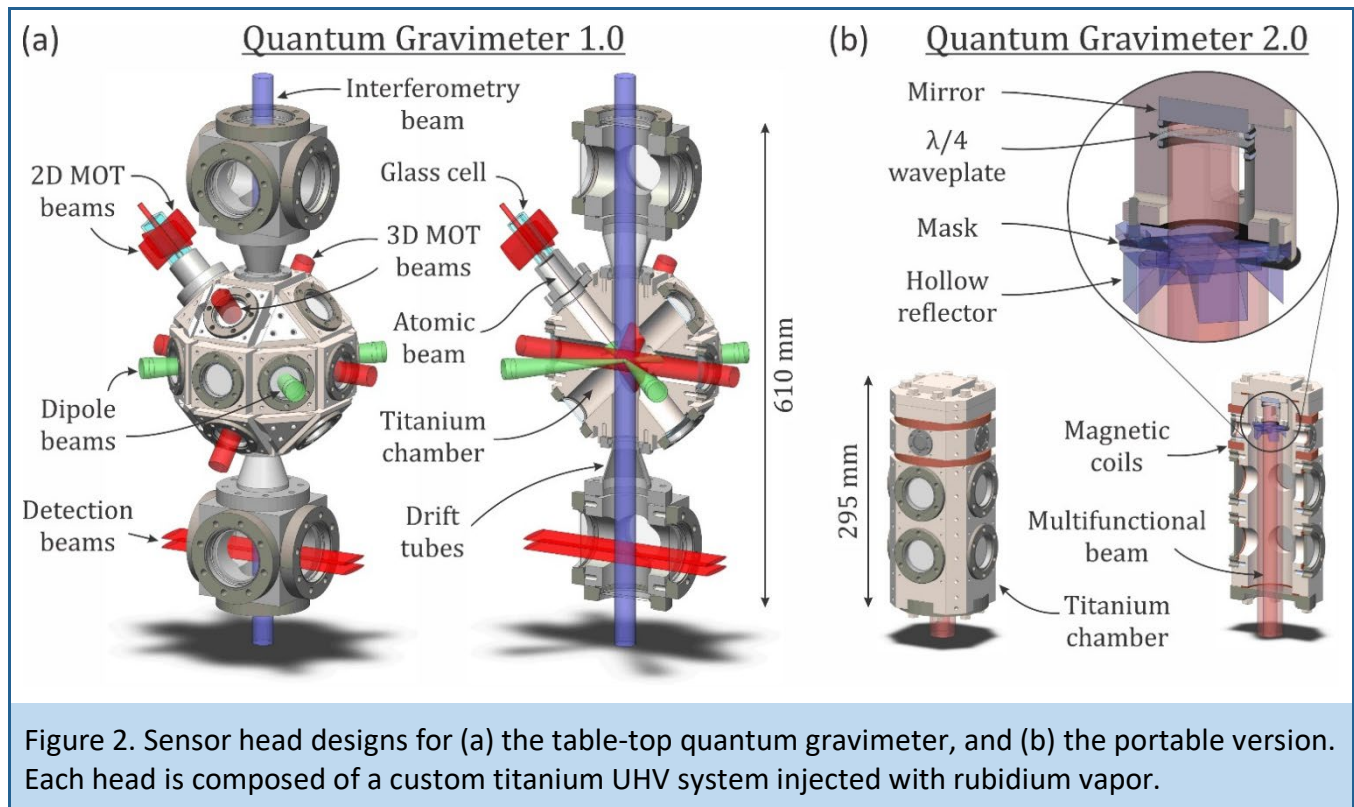


Figure 2. Sensor head designs for (a) the table-top quantum gravimeter, and (b) the portable version. Each head is composed of a custom titanium UHV system injected with rubidium vapor.

The science chamber is maintained at a lower pressure than the glass cell by virtue of differential pumping. This helps to avoid background fluorescence from rubidium vapor and will enable the use of evaporative cooling techniques [27] to reach sub-recoil temperatures. For this, we will use a high-intensity laser, red-detuned far below the D2 transitions in  $^{87}\text{Rb}$ , to create a crossed optical dipole trap [28]. Here, atoms are attracted to the high-intensity regions of the dipole beams due to the gradient of the optical potential [29]. By gradually lowering the trap depth, faster-moving atoms escape the trap while the remained atoms re-thermalize to a lower temperature. The use of “painted” optical potentials generated by rapidly moving beams can further increase the evaporation rate [30]—making sample temperatures  $< 10^{-7}$  K attainable in under 1 s of evaporation time. Ultra-cold atomic samples have been shown to dramatically improve the gravimeter’s sensitivity [31] and accuracy by reducing the dominant systematic effects due to laser wavefront distortion [32, 33].

Quantum Gravimeter 2.0 (QG2) is designed to be a compact, robust, and portable instrument. It consists of a 2.2-L all-titanium body with integrated magnetic coil frames and a 0.2-m-long drift tube. Several viewports allow for probing/imaging the atomic cloud at different positions. Central to the design is a custom in-vacuum hollow reflector that enables a single-laser-beam architecture for both cooling and interferometry [34, 8]. Figure 2(b) illustrates a large-diameter, circularly polarized laser beam incident on the reflector from the bottom. The hollow reflector consists of four right-angle prisms optically contacted to a baseplate and aligned in quadrants that reflect incident light twice by 90 degrees. The central part of the beam transmits through a square aperture at the center of the reflector. The beam then passes through a quarter waveplate and retro-reflects off a mirror fixed to the top of the chamber. This creates three mutually orthogonal pairs of counter-propagating beams within the hollow reflector. Each prism is covered with a high-reflection, zero-phase dielectric coating that maintains the direction of circular polarization at each reflection. Light propagating within the hollow reflector then creates the ideal  $\sigma^+/\sigma^-$  polarization required for a 3D MOT [35]. Below the hollow reflector, the atoms are exposed to only two counter-propagating vertical beams that have  $\sigma^+/\sigma^+$  or  $\sigma^-/\sigma^-$  polarization, which is ideal for driving velocity-sensitive Raman transitions in the interferometer [34].

QG2 is less than 1/3 the volume of QG1 and requires 1/10 the number of laser beams, which drastically reduces the instrument’s hardware complexity, size, weight, and power consumption. The trade-off is reduced experimental flexibility and free-fall height (maximum interrogation time  $T \approx 80$  ms). As a result, QG2 targets a more modest sensitivity of  $4 \times 10^{-8}$  g at 1 s, and an accuracy around  $5 \times 10^{-9}$  g. However, as a portable instrument designed to operate in relevant environments outside a climate-controlled laboratory, it will be competitive with other commercial absolute gravimeters [7, 9].

## CONCLUSION

Canada’s vast and resource-rich landscape demands advanced tools for precise geophysical and geodetic measurements. While classical gravimeters have long served this role, their limitations highlight the need for next-generation solutions. Quantum gravimeters offer a transformative alternative with their enhanced stability, reduced maintenance, and suitability for remote deployment. Despite international advances, Canada has yet to fully capitalize on this technology. The development

of quantum gravimeters at the University of New Brunswick marks a critical step toward establishing domestic capability in quantum sensing, supporting both scientific exploration and national strategic priorities.

## ACKNOWLEDGEMENTS

This work is supported by NSERC, CFI, NBIF, UNB, and the DND IDEaS program. We thank John Crowley of NRCan for inciteful feedback on the introduction. We also thank Franck Pereira Dos Santos, Baptiste Battelier, Bruno Desruelle, and Philippe Bouyer for helpful discussions.

## REFERENCES

1. X. Li, J. W. Crowley, S. A. Holmes, Y.-M. Wang, The contribution of the GRAV-D airborne gravity to geoid determination in the Great Lakes region, *Geophys. Res. Lett.* **43**, 4358–4365 (2016). <https://doi.org/10.1002/2016GL068374>
2. M. Van Camp, O. de Viron, A. Watlet, B. Meurers, O. Francis, and C. Caudron, Geophysics from terrestrial time-variable gravity measurements, *Rev. of Geophys.* **55**, 938-992 (2017). <https://doi.org/10.1002/2017RG000566>
3. D. Carbone, M. P. Poland, M. Diament, and F. Greco, The added value of time-variable microgravimetry to the understanding of how volcanoes work, *Earth-Sci. Rev.* **169**, 146 (2017). <https://doi.org/10.1016/j.earscirev.2017.04.014>
4. L. Antoni-Micollier, D. Carbone, V. Ménoiret, L. Lautier-Gaud, T. King, F. Greco, A. Messina, D. Contrafatto, and B. Desruelle, Detecting volcano-related underground mass changes with a quantum gravimeter, *Geophys. Res. Lett.* **49**, e2022GL097814 (2022). <https://doi.org/10.1029/2022gl097814>
5. A. Lambert, S. D. Pagiatakis, A. Billyard, and H. Dragert, Improved ocean tide loading corrections for gravity and displacement: Canada and northern United States, *J. of Geophys. Res. Solid Earth* **103**, 30231-30244 (1998). <https://doi.org/10.1029/98JB02735>
6. T. M. Niebauer, G. S. Sasagawa, J. E. Faller, R. Hilt, and F. Klopping, A new generation of absolute gravimeters, *Metrologia* **32**, 159 (1995). <https://doi.org/10.1088/0026-1394/32/3/004>
7. Micro-G LaCoste: A Division of LRS, Instruments (accessed May 2025). <https://microglacoste.com/shop/>
8. V. Ménoiret, P. Vermeulen, N. Le Moigne, S. Bonvalot, P. Bouyer, A. Landragin, and B. Desruelle, Gravity measurements below  $10^{-9} g$  with a transportable absolute quantum gravimeter, *Sci. Rep.* **8**, 12300 (2018). <https://doi.org/10.1038/s41598-018-30608-1>
9. Exail Ltd., Quantum gravimeters – ultra-high precision gravity measurements (accessed May 2025). <https://www.exail.com/product/quantum-gravimeters>
10. E. Janitz, P. Barclay, and L. Childress, Quantum Sensing in Canada, *Physics in Canada* **81**(2), 44 (2025).
11. B. Barrett, I. Chan, and A. Kumarakrishnan, Atom-interferometric techniques for measuring uniform magnetic field gradients and gravitational acceleration, *Phys. Rev. A* **84**, 063623, (2011). <https://doi.org/10.1103/PhysRevA.84.063623>
12. C. Mok, B. Barrett, A. Carew, R. Berthiaume, S. Beattie, and A. Kumarakrishnan, Demonstration of improved sensitivity of echo interferometers to gravitational acceleration, *Phys. Rev. A* **88**, 023614 (2013). <https://doi.org/10.1103/PhysRevA.88.023614>

13. B. Barrett, A. Carew, H. C. Beica, A. Vorozcovs, A. Pouliot, and A. Kumarakrishnan, Prospects for Precise Measurements with Echo Atom Interferometry, *Atoms* **4**, 19 (2016).  
<https://doi.org/10.3390/atoms4030019>
14. J. Le Gouët, T. E. Mehlstäubler, J. Kim, S. Merlet, A. Clairon, A. Landragin, and F. Pereira Dos Santos, Limits to the sensitivity of a low noise compact atomic gravimeter, *Appl. Phys. B: Lasers and Optics* **92**, 133-144 (2008). <https://doi.org/10.1007/s00340-008-3088-1>
15. X. Wu, Z. Pagel, B. S. Malek, T. H. Nguyen, F. Zi, D. S. Scheirer, and H. Müller, Gravity surveys using a mobile atom interferometer, *Sci. Adv.* **5**, 1–10, (2019).  
<https://doi.org/10.1126/sciadv.aax0800>
16. C. Li, L. Long, M. Huang, B. Chen, Y. Yang, X. Jiang, C. Xiang, Z. Ma, D. He, L. Chen, and S. Chen, Continuous gravity measurement with a portable atom gravimeter, *Phys. Rev. A* **108**, 032811 (2023). <https://doi.org/10.1103/PhysRevA.108.032811>
17. C. Freier, M. Hauth, V. Schkolnik, B. Leykauf, M. Schilling, H. Wziontek, H.-G. Scherneck, J. Muller, and A. Peters, Mobile quantum gravity sensor with unprecedented stability, *J. Phys. Conf. Ser.* **723**, 012050 (2016). <https://doi.org/10.1088/1742-6596/723/1/012050>
18. B. Stray, *et al.*, Quantum sensing for gravity cartography, *Nature* **602**, 590-594, (2022).  
<https://doi.org/10.1038/s41586-021-04315-3>
19. N. Shettell, K. S. Lee, F. E. Oon, E. Maksimova, C. Hufnagel, S. Wei, and R. Dumke, Geophysical survey based on hybrid gravimetry using relative measurements and an atomic gravimeter as an absolute reference, *Sci. Rep.* **14**, 6511, (2024). <https://doi.org/10.1038/s41598-024-57253-1>
20. Y. Bidel, N. Zahzam, C. Blanchard, A. Bonnin, M. Cadoret, A. Bresson, D. Rouxel, and M. F. Lequentrec-Lalancette, Absolute marine gravimetry with matter-wave interferometry, *Nature Comms.* **9**, 627 (2018). <https://doi.org/10.1038/s41467-018-03040-2>
21. Y. Bidel, N. Zahzam, A. Bresson, C. Blanchard, M. Cadoret, A. V. Olesen, and R. Forsberg, Absolute airborne gravimetry with a cold atom sensor, *J. Geodesy* **94**, 20 (2020).  
<https://doi.org/10.1007/s00190-020-01350-2>
22. M. Kasevich and S. Chu, Atomic interferometry using stimulated Raman transitions, *Phys. Rev. Lett.* **67**, 181 (1991). <https://doi.org/10.1103/PhysRevLett.67.181>
23. C. Antoine and Ch. Bordé, Exact phase shifts for atom interferometry, *Phys. Lett. A* **306**, 277-284 (2003). [https://doi.org/10.1016/S0375-9601\(02\)01625-0](https://doi.org/10.1016/S0375-9601(02)01625-0)
24. A. Peters, K. Y. Chung, and S. Chu, High-precision gravity measurements using atom interferometry, *Metrologia* **38**, 25 (2001). <https://doi.org/10.1088/0026-1394/38/1/4>
25. P. Gillot, O. Francis, A. Landragin, F. Pereira Dos Santos, and S. Merlet, Stability comparison of two absolute gravimeters: optical versus atomic interferometers, *Metrologia* **51**, L15 (2014).  
<https://doi.org/10.1088/0026-1394/51/5/L15>
26. J. Schoser, A. Batär, R. Löw, V. Schweikhard, A. Grabowski, Y. B. Ovchinnikov, and T. Pfau, Intense source of cold Rb atoms from a pure two-dimensional magneto-optical trap, *Phys. Rev. A* **66**, 023410 (2002). <https://doi.org/10.1103/PhysRevA.66.023410>
27. W. Ketterle, and N. J. van Druten, Evaporative Cooling of Trapped Atoms, in *Advances in Atomic, Molecular and Optical Physics Volume 37*, 181-236 (Academic Press, 1996).  
[https://doi.org/10.1016/S1049-250X\(08\)60101-9](https://doi.org/10.1016/S1049-250X(08)60101-9)
28. C. S. Adams, H. J. Lee, N. Davidson, M. Kasevich, and S. Chu, Evaporative cooling in a crossed dipole trap, *Phys. Rev. Lett.* **74**, 3577-3580, (1995).  
<https://doi.org/10.1103/PhysRevLett.74.3577>

29. J. D. Miller, R. A. Cline, and D. J. Heinzen, Far-off-resonance trapping of atoms, *Phys. Rev. A* **47**, R4567 (1993). <https://doi.org/10.1103/PhysRevA.47.R4567>
30. R. Roy, A. Green, R. Bowler, and S. Gupta, Rapid cooling to quantum degeneracy in dynamically shaped atom traps, *Phys. Rev. A* **93**, 043403 (2016). <https://doi.org/10.1103/PhysRevA.93.043403>
31. K. S. Hardman, P. J. Everitt, G. D. McDonald, P. Manju, P. B. Wigley, M. A. Sooriyabandara, C. C. N. Kuhn, J. E. Debs, J. D. Close, and N. P. Robins, Simultaneous precision gravimetry and magnetic gradiometry with a Bose-Einstein Condensate: A high precision, quantum sensor, *Phys. Rev. Lett.* **117**, 138501 (2016). <https://doi.org/10.1103/PhysRevLett.117.138501>
32. R. Karcher, A. Imanaliev, S. Merlet, and F. Pereira Dos Santos, Improving the accuracy of atom interferometers with ultracold sources, *New J. Phys.* **20**, 113041 (2018). <https://doi.org/10.1088/1367-2630/aaf07d>
33. L. Pagot, S. Merlet, and F. Pereira Dos Santos, Influence of optical aberrations on the accuracy of an atomic gravimeter, *Opt. Express* **33**, 18843 (2025). <https://doi.org/10.1364/OE.544378>
34. Q. Bodart, S. Merlet, N. Malossi, F. Pereira Dos Santos, P. Bouyer, and A. Landragin, A cold atom pyramidal gravimeter with a single laser beam, *Appl. Phys. Lett.* **96**, 134101 (2010). <https://doi.org/10.1063/1.3373917>
35. K. I. Lee, J. A. Kim, H. R. Noh, and W. Jhe, Single-beam atom trap in a pyramidal and conical hollow mirror, *Opt. Lett.* **21**, 1177 (1996). <https://doi.org/10.1364/ol.21.001177>